






Crustacean Exoskeletons for the Extraction and Mechanical Characterization of Chitin for Biomedical Applications

Exoesqueleto de crustáceos para la obtención y caracterización mecánica de Quitina en aplicaciones biomédicas

Martha E. Sevilla Abarca¹   Pablo R. Valle Velasco¹  María B. Paredes Robalino¹ 
Alejandra M. Lascano Moreta¹ 

¹ Universidad Técnica de Ambato. Ecuador Ambato.

Abstract

Introduction: In the field of biomedical applications, the use of biodegradable and biocompatible materials is essential. In this context, seafood shell waste represents an innovative and sustainable alternative for the production of biomaterials. This study addresses the use of shrimp and crab exoskeleton waste, which generates an unpleasant odor that affects the quality of life of residents in the center of Ambato city. The study highlights the need to investigate the mechanical properties of these exoskeletons for potential use in biomedicine, specifically in tissue engineering.

Objective: The objective of this study is to analyze the mechanical properties of shrimp and crab exoskeletons to evaluate their potential for chitin extraction and subsequent application in the biomedical field.

Materials and Methods: For chitin extraction, three types of exoskeleton species were used: brown shrimp, red shrimp, and crab, the most common in the region. The shells were washed to remove impurities, then dried and sieved. The resulting powder was stored in an airtight container. This powder was then used to produce chitin through a chemical process involving deproteinization with NaOH 0.1N and demineralization with HCl 0.1N. The obtained chitin was molded according to ASTM D638-10 and dried at room temperature.

Results: The material characterization showed that the obtained chitin had an irregular morphology with particles of different sizes, suggesting a complex structure and a larger surface area. The mechanical properties indicated that the material's hardness was 88.15 HD, classifying it as relatively hard. Additionally, the roughness measured 5.1 μm , and the tensile strength reached 7.43 MPa for brown shrimp, indicating that the material can withstand a significant amount of stress, making it suitable for biomedical applications.

Conclusions: The study demonstrates that shrimp and crab exoskeletons can be effectively utilized to obtain chitin, a biomaterial with mechanical properties suitable for biomedical applications such as tissue engineering. The highlighted properties, such as hardness and tensile strength, confirm its potential to be a useful material in this field.

Keywords: Chitin, deproteinization, demineralization, mechanical properties.

Resumen

Introducción: En el campo de las aplicaciones biomédicas, la utilización de materiales biodegradables y biocompatibles es esencial. En este contexto, los residuos de caparzones de mariscos representan una alternativa innovadora y sustentable para la producción de biomateriales. Este estudio aborda el aprovechamiento de los desechos de caparzones de camarón y cangrejo, los cuales generan un olor desagradable que afecta la calidad de vida de los habitantes en el centro de la ciudad de Ambato. Se destaca la necesidad de investigar las propiedades mecánicas de estos exoesqueletos para su posible uso en biomedicina, específicamente en la ingeniería de tejidos.

Objetivo: El objetivo de este estudio es analizar las propiedades mecánicas de los exoesqueletos de camarón y cangrejo, con el fin de evaluar su potencial para la obtención de quitina y su posterior aplicación en el ámbito biomédico.

Materiales y Métodos: Para la obtención de la quitina, se utilizaron tres tipos de especies de exoesqueletos: camarón marrón, camarón rojo y cangrejo, los cuales son los más comunes en la región. Los caparzones fueron lavados para eliminar impurezas, luego se secaron y se tamizaron. El polvo resultante se almacenó en un recipiente hermético. Posteriormente, se utilizó este polvo para la producción de quitina a través de un proceso químico que incluyó desproteinización con NaOH 0,1N y desmineralización con HCl 0,1N. La quitina obtenida fue moldeada siguiendo la norma ASTM D638-10 y secada a temperatura ambiente.

Resultados: La caracterización del material mostró que la quitina obtenida presenta una morfología irregular, con partículas de diferentes tamaños, lo que sugiere una estructura compleja y una mayor área superficial. Las propiedades mecánicas indicaron que la dureza del material fue de 88,15 HD, lo que clasifica al material como relativamente duro. Además, la rugosidad medida fue de 5,1 μm y el esfuerzo de tensión alcanzó 7,43 MPa para el camarón marrón, lo que indica que el material es capaz de soportar una cantidad significativa de estrés, lo cual es útil para aplicaciones biomédicas.

Conclusiones: El estudio demuestra que los exoesqueletos de camarón y cangrejo pueden ser utilizados de manera efectiva para la obtención de quitina, un biomaterial con características mecánicas adecuadas para aplicaciones biomédicas, como la ingeniería de tejidos. Las propiedades destacadas, como la dureza y la capacidad de soportar tensión, confirman su potencial para ser un material útil en este campo.

Palabras clave: Quitina, desproteinización, desmineralización, propiedades mecánicas

How to cite?

Sevilla M E, Valle PR, Paredes MB, Lascano A M. Utilization of Crustacean Exoskeletons for the Extraction and Mechanical Characterization of Chitin for Biomedical Applications. Ingeniería y Competitividad, 2025, 27(2) e-20114004

<https://doi.org/10.25100/iyv.v27i2.14004>

Received: 06/18/24

Reviewed: 09/25/24

Accepted: 02/24/25

Online: 04/9/25

Correspondence

marthaesevilla@uta.edu.ec



Spanish version



Contribution to the literature

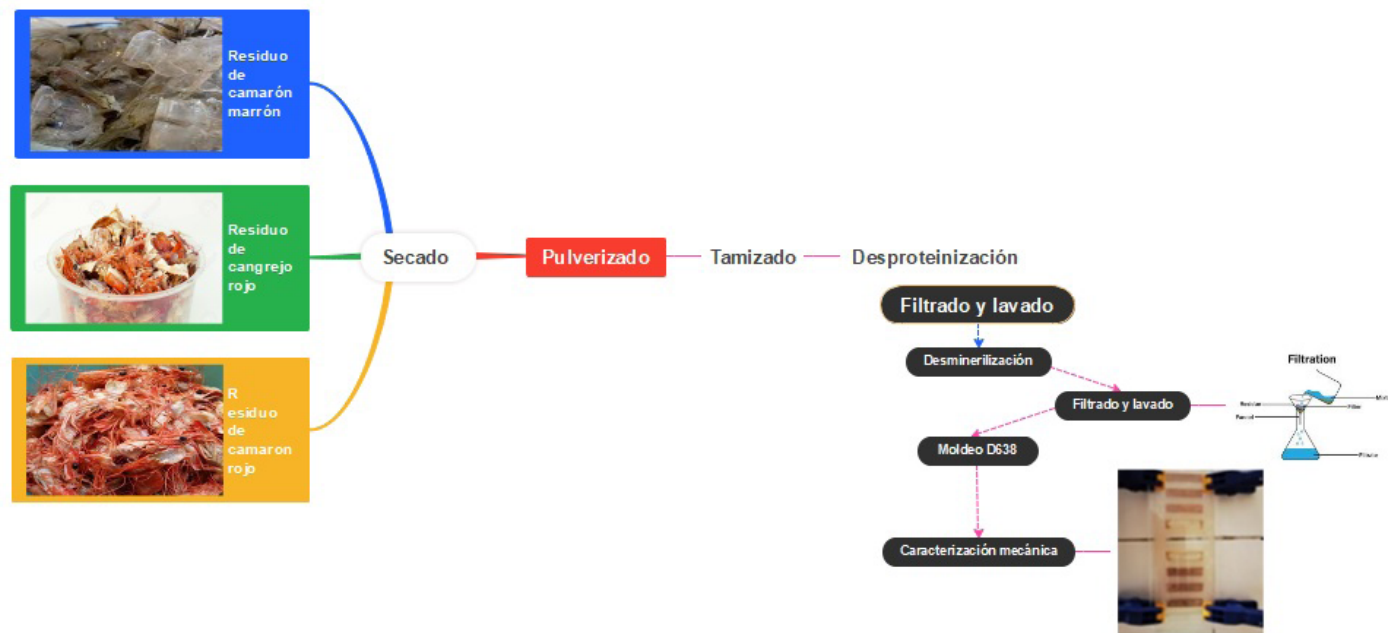
The study was conducted to extract chitin from shrimp and crab shells (abundant waste from the fishing industry) and to characterize its mechanical and microstructural properties. This research aims to explore sustainable methods for obtaining chitin and to evaluate its potential applications in fields such as biomaterials, packaging, and environmental remediation.

The most relevant results include:

The most relevant results showed that chitin extracted from shrimp and crab shells exhibits high purity, excellent mechanical properties (e.g., tensile strength, hardness, and roughness), and a well-defined microstructure.

These results contribute to the following:

These findings contribute to developing sustainable, high-performance materials for applications in biomedicine, packaging, and composite materials, highlighting the value of marine byproducts. The mechanical and microstructural characterization provides valuable data for designing chitin-based composites with tailored properties. In addition, surface roughness was measured, which is essential for applications such as coatings or biomedical implants.



Introduction

It is estimated that the global production of shrimp will reach approximately 5.6 million metric tons (MMT) in 2023. The five leading producers, namely Ecuador, China, India, Vietnam, and Indonesia, are expected to collectively contribute approximately 74% of the global production in 2023 (1). The shrimp processing industry generates around 3.8 million tons of waste annually on a global scale, which constitutes roughly 50-60% of the total catch volume (2).

The chitin content present in mollusc shells ranges from 8% to 40% (3), and this chemical compound has medical applications in the treatment of microbial infections and cancer (4). The hydrophilic character and antimicrobial properties of chitin are its most important applications, especially with regard to the production of new biomaterials (5). Chitosan and chitin are key substances in pharmaceutical formulations that have antimicrobial and antibacterial properties, and they also have antitumor activity against human monocytic leukemia cell lines (6). The majority of these applications necessitate highly purified chitin, underscoring the significant interest in optimizing its extraction to minimize impurities (7).

Chitin is a linear aminopolysaccharide consisting primarily of 2-acetamido-2-deoxy- β -D-glucopyranose units linked to β -(1-4) and partially of 2-amino-2-amino-2 units linked to β -(1-4)-deoxy- β -D-glucopyranose (8) (9) (10). It occurs naturally as three polymorphic modifications: α -, β -, and γ -chitin. α -Chitin is the most abundant form of chitin; it is found in the exoskeletons of insects and crustaceans. In contrast, the β -chitin is found in the squid feather, the body of tubeworms, and certain other sources. Notably, the γ -chitin, the least common and least studied polymorphic form of chitin, can be isolated from fungi in trace amounts (11) (12) (13). This biopolymer is composed of 2-acetamide-2-deoxy- β -D-glucose units linked by β -(1-4) bonds, and it can be readily obtained through chemical or biological treatment of crustacean waste (14) (15).

However, the extraction of chitin from all the aforementioned biological sources utilizes the same simple chemical treatment procedure, namely demineralization, deprotection, and decolorization (16). The storage of raw materials and the extraction of these components vary significantly, suggesting the need for process standardization. The distinctive features of chitosan, a natural polymeric sugar found primarily in the hard exoskeletons of various crustaceans (17), such as crabs, lobsters, and shrimp, are well-documented (14). It occurs in the form of ordered crystalline microfibrils that serve as structural components in various organisms, insects, and marine microorganisms (18). The chitin-glucan complex (CGC) is a primary component of the cell wall of fungi (19). Chitosan-based nanoparticles have found widespread use across a range of applications due to their advantageous properties, including biodegradability, high permeability, non-toxicity to humans, and cost-effectiveness (19). The use of novel quinine-based hydrogels has emerged as a promising avenue for new biomedical applications (20) (10). It has been identified as a protein source with significant biological activity, including antioxidant, antimicrobial, and antihypertensive properties (21).

Conversely, some consideration has been given to flame retardants that reduce the film-forming ability and mechanical properties of polymer coatings (22). The study utilized exoskeletons of shellfish such as *Farfantepenaeus californiensis* (brown shrimp), *Farfantepenaeus brevis*

(red shrimp), and Ecuadorian crab exoskeletons. The procedure for chitin extraction involves the removal of proteins and minerals by deproteinization and demineralization processes. The mechanical characteristics of the material are indicative of its reliability, including plasticity, fatigue, and fracture, which can lead to mechanical deterioration or failure. These characteristics are a direct result of the behavior of crystalline effects and are essential to improving and optimizing the mechanical properties of a material (23). The objective of the research is to obtain chitin from shellfish waste exoskeletons and to determine which biomaterial offers the favorable mechanical properties for biomedical applications. The article provides a comprehensive overview of the chitin production process, accompanied by in-depth analyses including mechanical characterization, microscopic examination, and infrared spectroscopic characterization of chitin.

Materials and metods

Materials and reagents, Chemical reagents

Biomass (shrimp exoskeletons: (shrimp-brown), (shrimp-red) and crab) from Ecuador, reagents: Hydrochloric acid 0.1 N Sigma Aldrich 37%, sodium hydroxide 0.1 N and distilled water.

Equipment

Precision mechanical convection oven is used to dry the sample, the (eco ball mill) is used to pulverize the sample, then it is passed through the controls sieve (also conf.to bs410nfx11501,504 uni 8620, din 4187, 4188), to obtain very fine particles. the thermo scientific magnetic stirrer is used for the chemical process of the material, acet.e1 shore durometer precision balance used to measure the hardness of the material, on the shore scale where 0 indicates a very low hardness and 100 a very high hardness.

For the test, ISO 868 (24) was used. Plastics and ebonite: determination of hardness by indentation using a type D Shore hardness tester. The Shore D hardness test is a non-destructive test that determines a material's resistance to penetration. It is commonly used for plastics and elastomers.

The procedure entails the selection of a flat, smooth sample of the material to be tested. Subsequently, a Shore D durometer is applied to the surface, exerting a defined force. The indenter penetrates the material, and the depth of penetration is measured on a graduated scale. This reading, expressed on the Shore D scale, provides a numerical value indicative of the material's hardness.

In order to obtain an accurate average result and ensure the representativeness of the data, it is imperative to perform a series of measurements at multiple points on the sample. For the purpose of this study, the portable Mitutoyo roughness meter, equipped with a removable probe, was utilized to conduct the rigorous test. The specimen was positioned on a horizontal surface, and the probe traversed the surface with a range of 16 millimeters and a measuring range of 360 micrometers (-200 μm + 160 μm) and a diamond probe ISO Standard 4287:1997 (E/F) (24).

The scanning electron microscope (SEM) of the brand VEGA TESCAN was utilized to obtain high-resolution images of the surface, allowing for the observation of fine details at the microscopic level. This instrument employs a 220V voltage, a tungsten filament, and a 30KV electron gun. In

addition, Fourier-transform infrared spectroscopy (FTIR) was employed using the PerkinElmer Model Spectrum Two instrument. The latter is equipped with an internal standard that is used to identify the peaks of the functional groups of chitin. The tensile testing machine (Shimadzu) has a maximum load capacity of 50 kN and a force equivalent to 101.97 kilograms force. It is used to perform tensile tests on materials, allowing for the evaluation of their mechanical properties, such as resistance, ductility, and elastic limit. The tensile test is performed at a rate of 1 mm/min, in accordance with the standard D638. The test utilizes flat grips with an opening measuring between 0 and 7 mm. The machine operates at an input voltage of 220 V and a maximum load capacity of 50 kN. Figure 1.

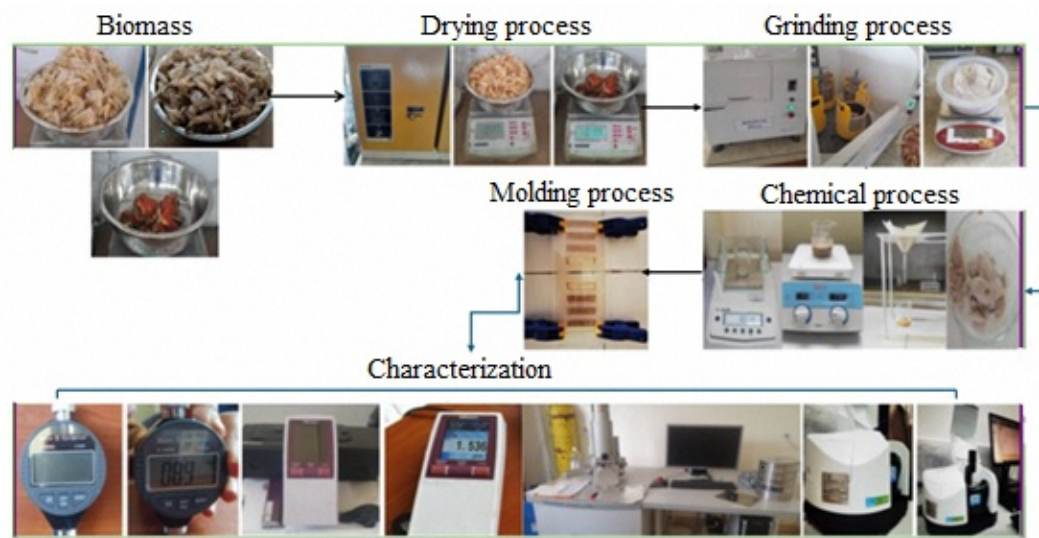


Figure. 1 Diagram of the process of obtaining Chitin

Chitin Production

A collection of shellfish exoskeletons was obtained from the central region of Ambato, meticulously categorized according to their taxonomic classification: *Farfantepenaeus californiensis* (C1) (brown shrimp), *Farfantepenaeus brevisrostris* (C2) (red shrimp), and *Brachyura* (C3) (crab). The shells were meticulously washed with ample water to eliminate any residual meat or impurities. They were then stored in hermetic containers to maintain their freshness and prevent contamination. The samples were stored at a temperature of -20°C . The weights utilized are enumerated in Table 1 below.

Table 1 Biomass of the fresh exoskeleton - dry biomass

Exoesqueleto	Biomasa en fresco (g)	Biomasa seca (g) T(60 $^{\circ}\text{C} \approx t = 24\text{h}$)
C1(camarón marrón)	1397	547
C2 (camarón rojo)	412	306
Exoesqueleto	Biomasa en fresco (g)	Biomasa seca (g) T(65 $^{\circ}\text{C} \approx t = 24\text{h}$)
C3 (cangrejo)	348	199

Subsequently, samples C1 and C2 were milled at a speed of 520 rpm for 6 hours, while C3 was left for 24 hours due to its notably robust shell. The base weight of the ground-based shrimp sample is 490.1 g. Subsequently, the powders from samples C1, C2, and C3 were meticulously sieved using a standard sieve (DIN 4187, 4188) and stored in hermetic plastic containers to ensure their preservation. Subsequently, an amount of 8 g of shrimp waste is measured, crushed, and sieved. The waste is then subjected to a process of deproteinization with sodium hydroxide (NaOH) at a concentration of 0.1 N, with a solid-to-liquid ratio of 1:15. Thereafter, mineralization is conducted with HCl (0.1 N) at a ratio of (1:15) at a temperature of 40°C for a duration of 6 hours (25) (26). The samples are then thoroughly washed with ample water. The obtained chitin is then placed in molds with dimensions according to the standard ASTM D638 - 10, which refers to the "Standard Test Method for Determining the Tensile Properties of Plastics" (27).

Results and discussion

Characterization of chitin

For scanning electron microscopy, a dry sample was obtained following the demineralization and deproteinization procedures at an ambient temperature of 21.3°C and a relative humidity of 57.1%.

Scanning Electron Microscopy Analysis

The chitin sample, which has undergone preliminary drying and pulverization, is subsequently placed in the microscope chamber for analysis at room temperature. At a resolution of 500 μm , an irregular morphology is observed in Figure 2a, characterized by a difference in particle sizes that vary from (1017.41 μm - 251.69 μm) with agglomerations on the surface. These irregular particles have a large surface area (28) (29) and are more tractive with a probability of reacting with each other (30). Figure 2b presents a microstructure where agglomerations of the biomaterial with irregular geometry are observed with distances ranging from 31.66 μm to 1007.69 μm . These large and small particles generate greater anchorage in the biomaterial (31), but also promote biological interactions for the success of implants and medical devices.

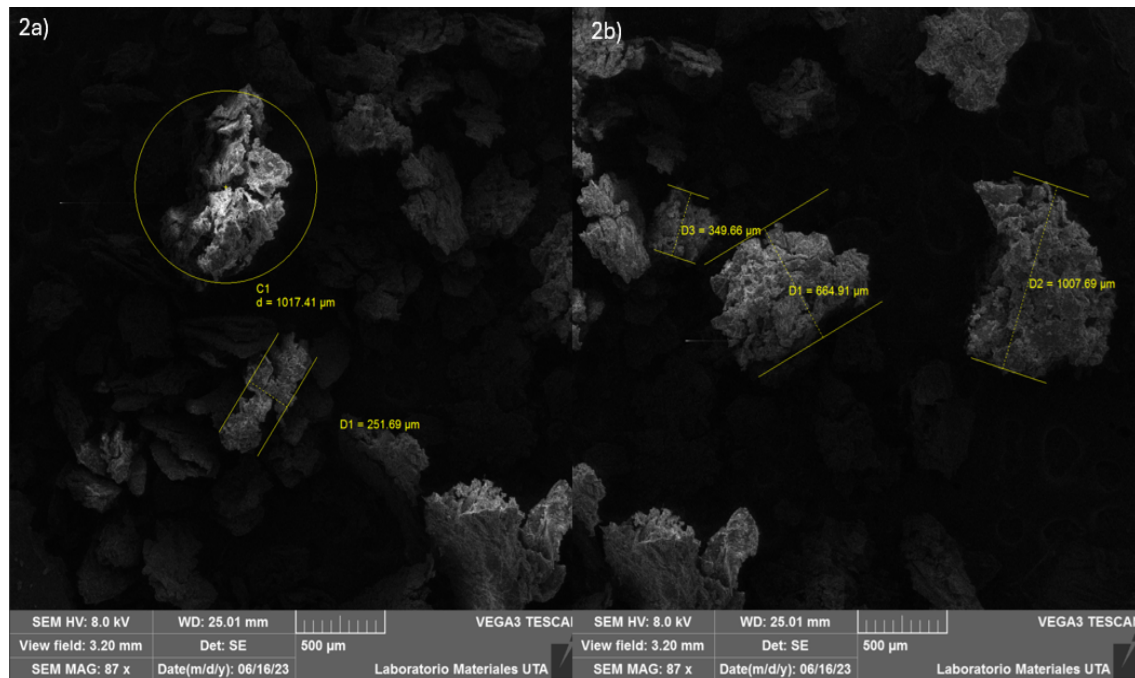


Figure. 2a, 2b. Scanning electron microscopy (SEM) of brown shrimp chitin

As illustrated in Figures 3a and 3b, the dried and pulverized sample of red shrimp chitin displays a rough morphology, characterized by irregular blocks with porosities and cavities measuring $27.73 \mu\text{m}$. This morphology suggests the utilization of ammonium, resulting in a complex structure that potentially impacts the functional characteristics of the biomaterial. The formation of porous structures leads to a reduction in material resistance. The influence of porosity on the location of stresses is further evidenced by the findings reported in research (32).

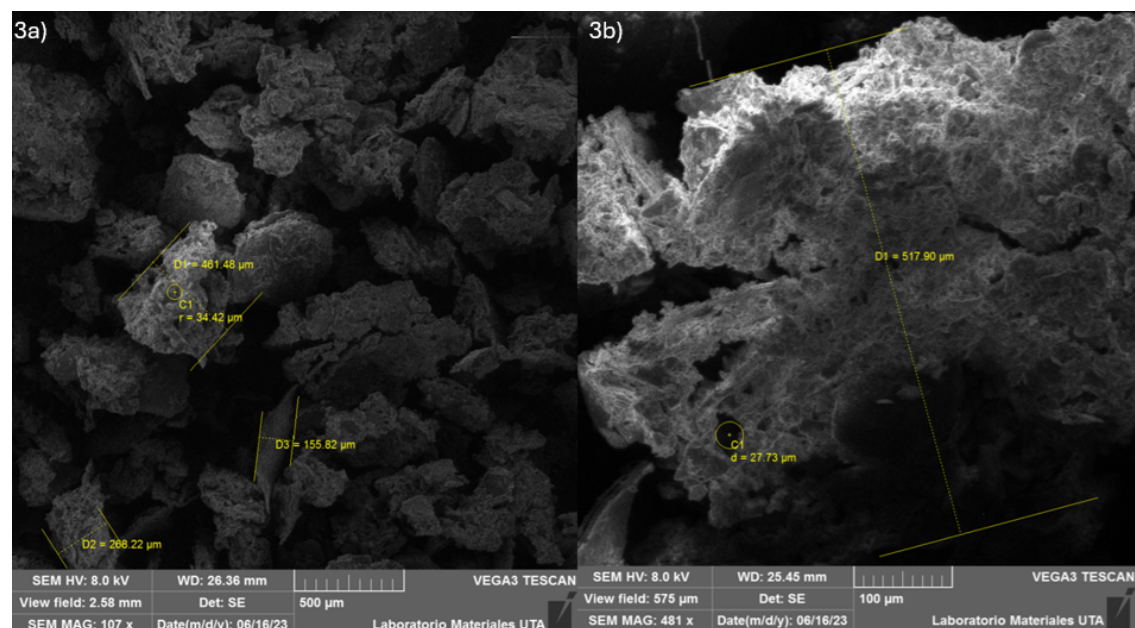


Figure. 3a, 3b. Scanning electron microscopy (SEM) of red shrimp chitin

FTIR Analysis

The three chitin samples were characterized using the KBr disk method in a FTIR spectrometer. Two spectrophotometers with a frequency range of (4000-400) cm^{-1} were utilized, and the zero samples of the species were analyzed. The peaks of the spectra were examined to identify the functional groups.

As illustrated in Figure 4, the peak at 3275.23 cm^{-1} , corresponding to NH and OH, is observed in the region of 3600-3500 cm^{-1} . This peak is indicative of the stretching of NH, characteristic of the amide group, as observed in the zero sample of the brown shrimp. Referencing (32) and (33), this finding is further corroborated. In the band (2924.76-2329.6) cm^{-1} , the presence of symmetric and asymmetric stretching (CH and CH₃ rings) is evident. The band (1552.58-1620) cm^{-1} exhibits characteristic peaks (1640.2 - 1520.3) cm^{-1} , corresponding to amides I and amides II. This observation indicates the presence of C-O-O and C = O bonds, facilitated by the presence of hydrogen bonds. Between the region (1300 - 800) cm^{-1} , characteristic peaks of 1025.4 cm^{-1} corresponding to CO are observed, and the floor at 865.3 cm^{-1} is attributed to the stretching of CO and the oxygen bridge.

In the region (1070-1025) cm^{-1} , a peak at 1025 cm^{-1} is observed, with signals attributed to the (CO of the COH ring characteristic of the saccharide structure). In the band (960-875) cm^{-1} , a peak at 865 cm^{-1} of the carboxyl dimer is observed (34). Furthermore, a substantial variation in the absorption ratios between the zero sample and the brown shrimp chitin sample is evident, which is attributed to structural alterations in the biomaterial.

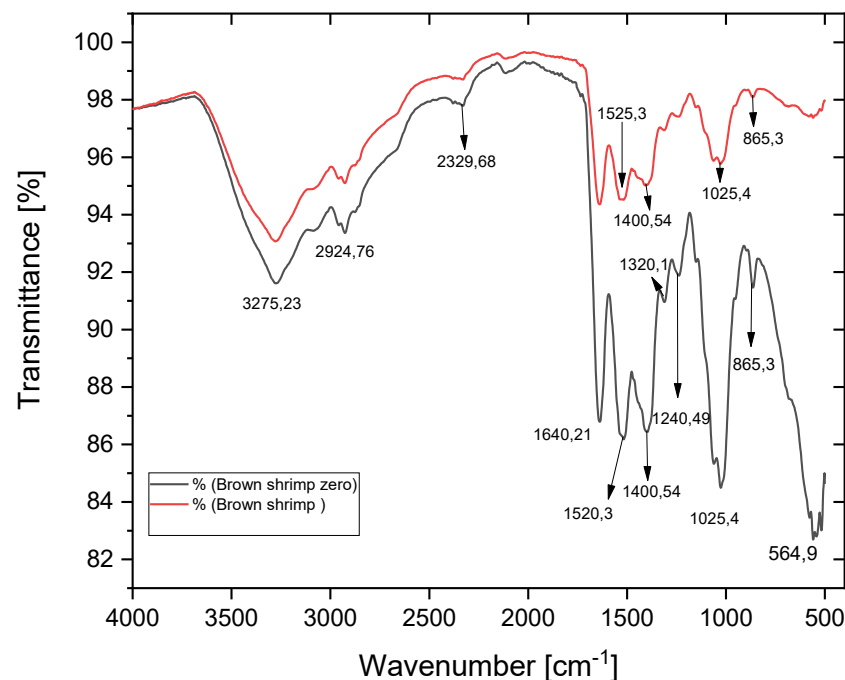


Figure. 4 FTIR analysis of the zero sample and the brown shrimp sample C1

As illustrated in Figure 5, the absorption peaks between sample zero and sample C2 (red shrimp) exhibit peaks (3059.6 - 3266.9) cm^{-1} that are characteristic of the band (3600 - 3500) cm^{-1} functional groups NH and OH. The peaks (2379.7 - 2129.3) demonstrate symmetric interactions CH and CH₃. The 1630-1315.1 cm^{-1} region corresponds to a carbonyl group, and the 1025 region exhibits a peak attributed to the CO of the COH ring. Between the band (960-875) cm^{-1} peaks of (880.16 - 685.6) cm^{-1} , a peak of 560 cm^{-1} is observed in the carboxyl band, indicative of out-of-plane torsion of the monomer. The variation in the proportions between the zero sample and the red shrimp chitin highlights a higher absorption in the red shrimp chitin, decreasing the peaks of the amides in addition to the signals corresponding to the stretching of the CO. This significant increase in the absorbance is attributed to the change in the biometry structures (35).

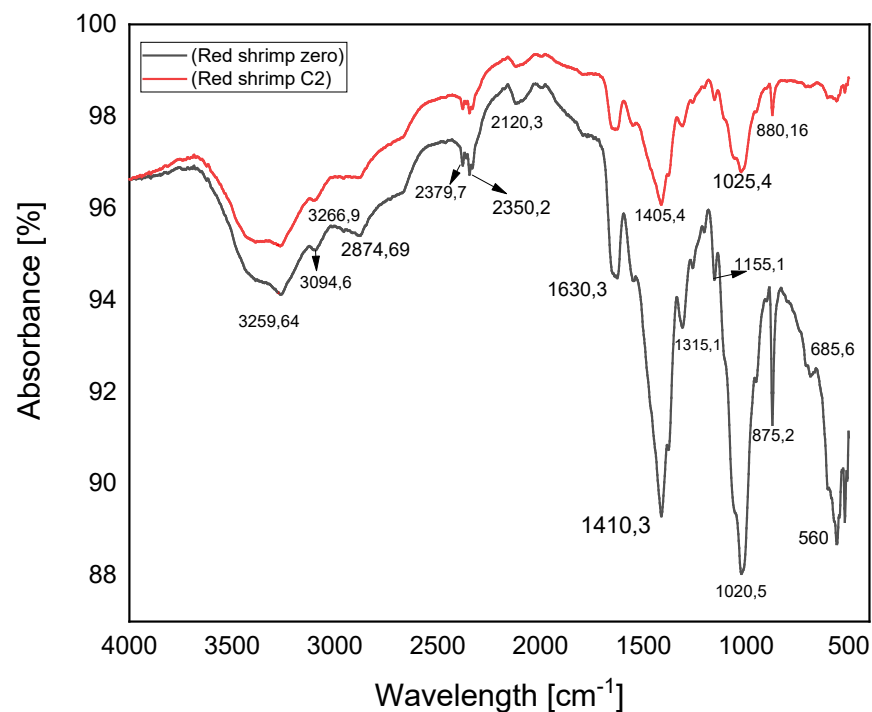


Figure. 5 FTIR analysis of the zero sample and the red shrimp sample C2

As illustrated in Figure 6, the zero crab sample and the crab chitin sample (C3) exhibit characteristic peaks within the region of 3275.4 to 3284.9 cm^{-1} , corresponding to NH and OH due to the stretching of the amide group. A peak at 2945 cm^{-1} , is observed, indicative of CH stretching. The bands (1405.4 - 1315.1) cm^{-1} , exhibit the groups corresponding to amides I and II, while a peak of 1399.3 cm^{-1} , is observed in the region of the asymmetric band of the carbonyl group. Between the bands (1300 - 800) cm^{-1} , a peak at 1029.8 cm^{-1} , is observed, corresponding to the carbonyl groups of the oxygen bridge, which are characteristic of the saccharide structure. In the band (584.6 - 563.8) cm^{-1} , there are plane alterations in the carboxyl dimer. The variations in the three samples' absorbances are indicative of the bending of the amide, involving the C-O stretching that are characteristic of the saccharide structure (36) (37) (38).

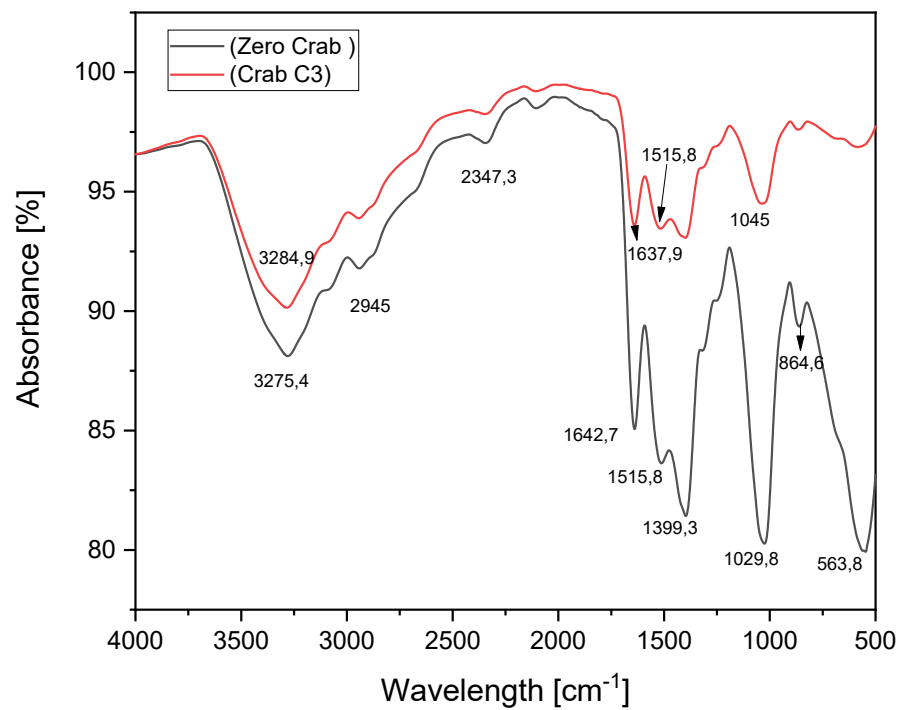


Figure. 6 FTIR analysis of the zero sample and the red shrimp sample C2

Hardness analysis

As illustrated in Figure 7, the hardness test of the dry chitin plate was conducted at a temperature of 21°C. A comparative analysis of the obtained data is presented in Table 2, which provides the average hardness of samples C1, C2, and C3.

Table 2. Comparison of hardness averages (HD)

Muestra	Promedio (HD)	ϑ
C1(camarón marrón)	88,150	0,944
C2 (camarón rojo)	75,01	2,436
C3 (cangrejo)	86,82	3.20

The mean chitin hardness of brown shrimp (87.475; 88.825) at a 95% confidence interval is presented in Table 3.

Table 3. Confidence interval for brown shrimp C1, mean hardness values

T of a sample: C1

N	Media	Desv. Est.	Error estándar de la media	IC de 95% para μ
10	88.15	0.944	0.299	(87.475; 88.825)

μ : *media de C1*

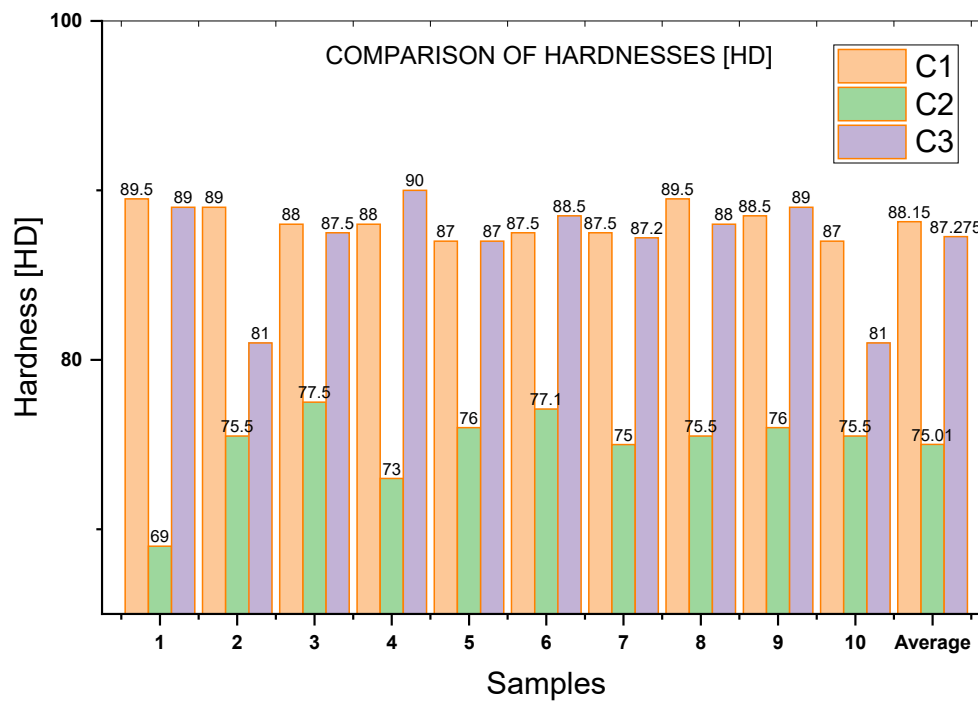


Figure. 7 Comparison of Hardnesses

Rigor Analysis

The roughness test is performed on each dry plate of the three species at room temperature. This test involves the use of a profilometer, which is a device that can record surface topography. The profilometer is moved over the surface to be examined, and as it advances, it records the vertical deviations of the surface with respect to a mean line. The data obtained are processed to obtain roughness parameters, such as average roughness. This parameter provides quantitative information on the surface texture, which is essential to evaluate the functional performance, finish, and quality of a part. As demonstrated in Figure 8, a comparison of the data obtained with the average roughness of the three samples (C1, C2, C3) reveals that sample C1 exhibits the highest roughness, with a value of $5.1 \mu\text{m}$, while sample C3 demonstrates the lowest roughness, with a value of $0.3 \mu\text{m}$.

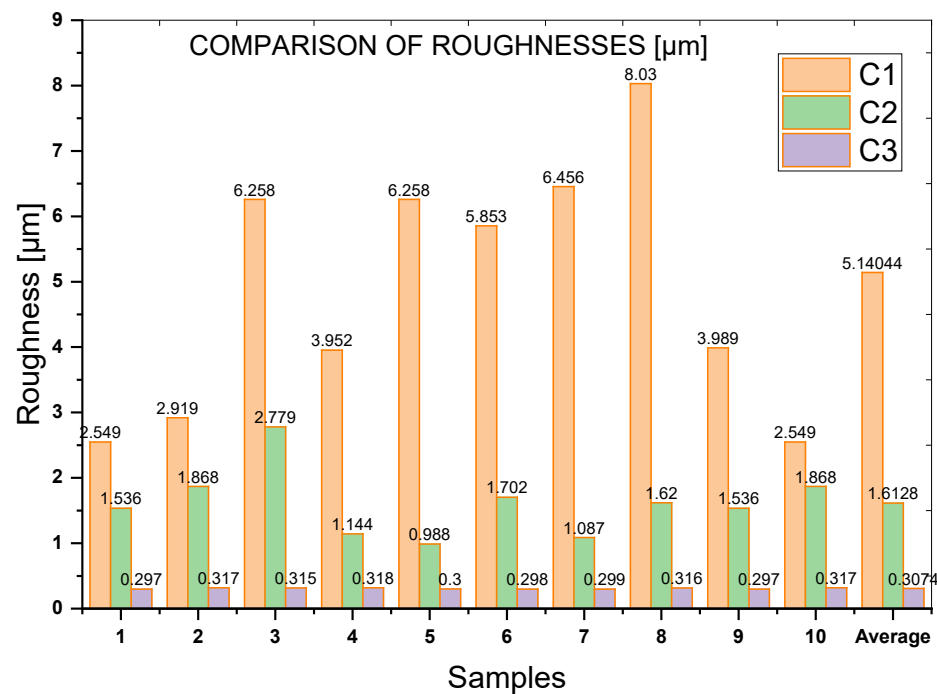


Figure. 8 Comparison of Roughness

Stress Analysis

As illustrated in Figure 9, a stress-strain curve derived from a mechanical test conducted on six specimens is presented. Specimen 1 demonstrates the highest peak with a maximum stress of approximately 7 MPa. It exhibits a substantial decline in stress following the peak, subsequently attaining a stable state that persists up to a strain of approximately 1.0%. This signifies a more ductile behavior. Specimen 2 demonstrates a maximum stress of approximately 5.5 MPa. However, following the peak, a rapid and more pronounced drop is observed, indicating a more brittle behavior due to the absence of a significant stable deformation phase. In contrast, specimen 3 exhibits a maximum stress of approximately 7.2 MPa. Nonetheless, the post-peak drop is less abrupt, suggesting a slight ductility prior to the final fracture. The fourth specimen exhibited a maximum stress of approximately 7.5 MPa, followed by a rapid decline, yet it demonstrated a slight load capacity at minimal deformation. Specimens 5 and 6, with a maximum stress of approximately 3.5 MPa, exhibited a rapid drop, suggesting potential early fracture or a defect in the specimen. The observed variations in the graphs could be attributed to the intrinsic properties of the material, defects in the specimens, or differences in the test conditions.

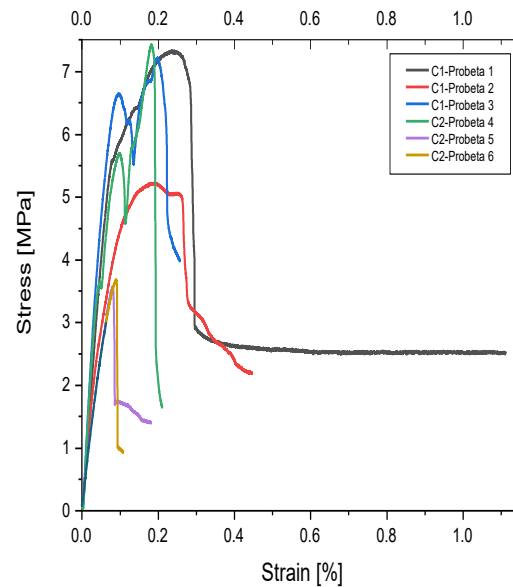


Figure. 9 Stress-strain curves of chitin Brown shrimp

As illustrated in Figure 10, the material initially exhibits elastic behavior, followed by a maximum strength of approximately 4.6 MPa and a significant degree of ductility after the stress drop. Although the material experiences a reduction in load capacity after the maximum peak, it maintains a constant residual capacity of approximately 3 MPa, rendering it suitable for applications that necessitate controlled plastic deformation prior to fracture. The maximum strain recorded was approximately 12%, suggesting the material's capacity to absorb energy prior to complete failure (crab).

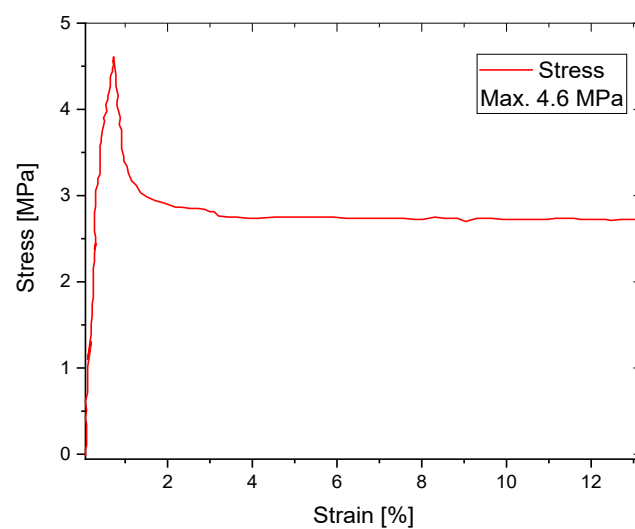


Figure 10. Stress-strain curves of red shrimp chitin



A review of the extant studies on chitin reveals an average tensile strength ranging from 1.3 to 8.48 MPa (26). The findings of the present study demonstrate a concurrence with the extant literature.

Conclusions

The initial method yielded chitin with agglomerations, while the method with 2% acetic acid yielded a single chitin fiber.

The tensile test results of the biopolymer align with the proposed requirements in the literature, with approximate values ranging from 7.5 to 4.6 MPa. In practical applications, materials exhibiting behavior analogous to that depicted in Figure 7 are particularly well-suited for structures necessitating controlled plastic deformation prior to fracturing. However, the observed variability in Figure 6 underscores the crucial role of stringent quality control measures to ensure material consistency.

The FTIR results identify the functional groups of amides I and II CO-NH, corresponding to chitin.

CRedit authorship contribution statement

Conceptualization - Ideas: Pablo Valle Velasco, Martha Sevilla Abarca. **Data Curation:** Pablo Valle Velasco, Martha Sevilla Abarca. **Formal analysis:** Pablo Valle Velasco, Martha Sevilla Abarca, Alejandra Lascano Moreta, María Paredes Robalino. **Acquisition of funding:** Pablo Valle Velasco, Martha Sevilla Abarca, Alejandra Lascano Moreta, María Paredes Robalino. **Investigation:** Pablo Valle Velasco, Martha Sevilla Abarca, Alejandra Lascano Moreta, María Paredes Robalino. **Methodology:** Pablo Valle Velasco, Martha Sevilla Abarca, Alejandra Lascano Moreta, María Paredes Robalino. **Project Management:** Pablo Valle Velasco, Martha Sevilla Abarca. **Resources:** Pablo Valle Velasco, Martha Sevilla Abarca, Alejandra Lascano Moreta, María Paredes Robalino. **Software:** Pablo Valle Velasco, Martha Sevilla Abarca, Alejandra Lascano Moreta, María Paredes Robalino. **Supervision:** Pablo Valle Velasco, Martha Sevilla Abarca. **Validation:** Pablo Valle Velasco, Martha Sevilla Abarca. **Visualization - Preparation:** Pablo Valle Velasco, Martha Sevilla Abarca. **Writing - original draft - Preparation:** Pablo Valle Velasco, Martha Sevilla Abarca. **Writing - revision and editing - Preparation:** Pablo Valle Velasco, Martha Sevilla Abarca.

Financing: Universidad Técnica de Ambato – Ecuador. **Conflict of interest:** does not declare.

Ethical aspect: does not declare.

References

- (1) W. Su, W. Xu, N. E. Polyakov, A. V Dushkin, P. Qiao, and W. Su, "Zero-waste utilization and conversion of shrimp shell by mechanochemical method," *J. Clean. Prod.*, vol. 425, no. September, p. 139028, 2023, <https://doi.org/10.1016/j.jclepro.2023.139028>
- (2) N. Rossi, C. Grosso, and C. Delerue-Matos, "Shrimp Waste Upcycling: Unveiling the Potential of Polysaccharides, Proteins, Carotenoids, and Fatty Acids with Emphasis on Extraction Techniques and Bioactive Properties," *Mar. Drugs*, vol. 22, no. 4, 2024, <https://doi.org/10.3390/md22040153>
- (3) D. Vadivel et al., "Innovative chitin-glucan based material obtained from mycelium of wood decay fungal strains," *Heliyon*, vol. 10, no. 7, p. e28709, 2024, <https://doi.org/10.1016/j.heliyon.2024.e28709>



- (4) S. Kumari and P. K. Rath, "Extraction and Characterization of Chitin and Chitosan from (Labeo rohita) Fish Scales," *Procedia Mater. Sci.*, vol. 6, no. Icmpec, pp. 482-489, 2014, <https://doi.org/10.1016/j.mspro.2014.07.062>
- (5) I. Younes and M. Rinaudo, "Chitin and Chitosan Preparation from Marine Sources. Structure, Properties and Applications," pp. 1133-1174, 2015, <https://doi.org/10.3390/md13031133>
- (6) M. Eddy, B. Tbib, and K. EL-Hami, "A comparison of chitosan properties after extraction from shrimp shells by diluted and concentrated acids," *Heliyon*, vol. 6, no. 2, p. e03486, 2020, <https://doi.org/10.1016/j.heliyon.2020.e03486>
- (7) C. Pedrazzani, L. Righi, F. Vescovi, L. Maistrello, and A. Caligiani, "Black soldier fly as a New chitin source: Extraction, purification and molecular/structural characterization," *Lwt*, vol. 191, no. July 2023, p. 115618, 2024, <https://doi.org/10.1016/j.lwt.2023.115618>
- (8) N. H. K. Al Shaqsi, H. A. S. Al Hoqani, M. A. Hossain, and M. A. Al Sibani, "Optimization of the demineralization process for the extraction of chitin from Omani Portunidae segnis," *Biochem. Biophys. Reports*, vol. 23, no. July, p. 100779, 2020, <https://doi.org/10.1016/j.bbrep.2020.100779>
- (9) J. Kumirska et al., "Application of spectroscopic methods for structural analysis of chitin and chitosan," *Mar. Drugs*, vol. 8, no. 5, pp. 1567-1636, 2010, <https://doi.org/10.3390/md8051567>
- (10) C. Chen et al., "Mechanically strong all-chitin filaments: Wet-spinning of β -chitin nanofibers in aqueous NaOH," *Int. J. Biol. Macromol.*, vol. 222, no. PB, pp. 3243-3249, 2022, <https://doi.org/10.1016/j.ijbiomac.2022.10.096>
- (11) E. Podgorbunskikh, T. Kuskov, V. Bukhtoyarov, O. Lomovsky, and A. Bychkov, "Recrystallization of Cellulose, Chitin and Starch in Their Individual and Native Forms," *Polymers (Basel)*, vol. 16, no. 7, 2024, <https://doi.org/10.3390/polym16070980>
- (12) W. G. Birolli, J. A. D. M. Delezuk, and S. P. Campana-Filho, "Ultrasound-assisted conversion of alpha-chitin into chitosan," *Appl. Acoust.*, vol. 103, pp. 239-242, 2016, <https://doi.org/10.1016/j.apacoust.2015.10.002>
- (13) T. Di Nardo and A. Moores, "Mechanochemical amorphization of chitin: Impact of apparatus material on performance and contamination," *Beilstein J. Org. Chem.*, vol. 15, pp. 1217-1225, 2019, <https://doi.org/10.3762/bjoc.15.119>
- (14) H. El Knidri, R. Belaabed, A. Addaou, A. Laajeb, and A. Lahsini, "Extraction, chemical modification and characterization of chitin and chitosan," *Int. J. Biol. Macromol.*, vol. 120, pp. 1181-1189, 2018, <https://doi.org/10.1016/j.ijbiomac.2018.08.139>
- (15) H. C. Curbelo and D. Y. Palacio, "Tratamiento químico de residuos de camarón para la obtención de quitina," *Rev. Cent. Azucar*, vol. 48, no. 2, pp. 103-116, 2021. http://scielo.sld.cu/scielo.php?pid=S2223-48612021000200103&script=sci_arttext
- (16) R. J. Camargo-Amado, M. E. Sevilla-Abarca, R. J. Camargo-Amado, and M. E. Sevilla-Abarca, "Chemical functionalization method to obtain graphene oxide adhered to the surface of high-density pyrolytic graphite plates by acid spray coating," *Ing. y Compet.*, vol. 23, no. 2, p. e21110838, 2021, <https://doi.org/10.25100/iyc.v23i2.10838>
- (17) B. Adegbemiro, S. Pathania, J. Wilson, B. Duffy, J. Maria, and C. Frias, "Extraction , quantification , characterization , and application in food packaging of chitin and chitosan from mushrooms : A review," vol. 237, no. March, 2023. <https://doi.org/10.1016/j.ijbiomac.2023.124195>
- (18) H. Ali Said Al Hoqani, N. Hamed Khalifa Al Shaqsi, M. Amzad Hossin, and M. Abdullah Al Sibani, "Structural characterization of polymeric chitosan and mineral from Omani shrimp shells," *Water-Energy Nexus*, vol. 4, pp. 199-207, 2021, <https://doi.org/10.1016/j.wen.2021.11.002>



- (19) A. Khayrova, S. Lopatin, y V. Varlamov, "Obtaining chitin, chitosan and their melanin complexes from insects", *Int. J. Biol. Macromol.*, vol. 167, no xxx, pp. 1319-1328, 2021. <https://doi.org/10.1016/j.ijbiomac.2020.11.086>
- (20) Y. Zou et al., "Biocompatible and biodegradable chitin-based hydrogels crosslinked by BDDE with excellent mechanical properties for effective prevention of postoperative peritoneal adhesion," *Carbohydr. Polym.*, vol. 305, <https://doi.org/10.1016/j.carbpol.2023.120543>
- (21) G. Yuan, Y. Pan, W. Li, C. Wang, and H. Chen, "Effect of extrusion on physicochemical properties, functional properties and antioxidant activities of shrimp shell wastes protein," *Int. J. Biol. Macromol.*, vol. 136, pp. 1096-1105, 2019, <https://doi.org/10.1016/j.ijbiomac.2019.06.145>
- (22) S. Batool, W. Guo, R. Gill, W. Xin, and Y. Hu, "Chitin based multi-layered coatings with flame retardancy an approach to mimic nacre: Synthesis, characterization and mechanical properties," *Carbohydr. Polym.*, vol. 291, no. May 2021, 2022, <https://doi.org/10.1016/j.carbpol.2022.119488>
- (23) E. Farina et al., "Micro computed tomography based finite element models for elastic and strength properties of 3D printed glass scaffolds," *Acta Mech. Sin. Xuebao*, vol. 37, no. 2, pp. 292-306, 2021, <https://doi.org/10.1007/s10409-021-01065-3>
- (24) S. Fooladi y S. R. Kiahosseini, "Creation and investigation of chitin/HA double-layer coatings on AZ91 magnesium alloy by dipping method", *J. Mater. Res.*, vol. 32, no 13, pp. 2532-2541, 2017. <https://doi.org/10.1557/jmr.2017.231>
- (25) M. D. C. D et al., "Chitin nanowhiskers from shrimp shell waste as green filler in acrylonitrile-butadiene rubber : Processing and performance properties," *Carbohydr. Polym.*, vol. 245, no. May, p. 116505, 2020, <https://doi.org/10.1016/j.carbpol.2020.116505>
- (26) L. Ilijin et al., "Sourcing chitin from exoskeleton of *Tenebrio molitor* fed with polystyrene or plastic kitchen wrap", *Int. J. Biol. Macromol.*, vol. 268, no March, 2024. <https://doi.org/10.1016/j.ijbiomac.2024.131731>
- (27) M. Ast, "D638, Standard test method for tensile properties of plastics," *TF_~ VFING HOOP TENSILE l'REN ...*, no. C, pp. 1-16, 2013, doi: 10.1520/D0638-10.1.
- (28) S. Islam, M. A. R. Bhuiyan, and M. N. Islam, "Chitin and Chitosan: Structure, Properties and Applications in Biomedical Engineering," *J. Polym. Environ.*, vol. 25, no. 3, pp. 854-866, 2017, <https://doi.org/10.1007/s10924-016-0865-5>
- (29) S. Peter, N. Lyczko, D. Gopakumar, H. J. Maria, A. Nzihou, and S. Thomas, "Chitin and Chitosan Based Composites for Energy and Environmental Applications: A Review," *Waste and Biomass Valorization*, vol. 12, no. 9, pp. 4777-4804, 2021, <https://doi.org/10.1007/s12649-020-01244-6>
- (30) M. Ul-Islam, K. F. Alabbosh, S. Manan, S. Khan, F. Ahmad, and M. W. Ullah, "Chitosan-based nanostructured biomaterials: Synthesis, properties, and biomedical applications," *Adv. Ind. Eng. Polym. Res.*, vol. 7, no. 1, pp. 79-99, 2024, <https://doi.org/10.1016/j.aiepr.2023.07.002>
- (31) M. G. García, J. Marchese, and N. A. Ochoa, "Effect of the particle size and particle agglomeration on composite membrane performance," *J. Appl. Polym. Sci.*, vol. 118, no. 4, pp. 2417-2424, 2010, <https://doi.org/10.1002/app.32274>
- (32) H. El Knidri, R. El Khalfaouy, A. Laajeb, A. Addaou, and A. Lahsini, "Eco-friendly extraction and characterization of chitin and chitosan from the shrimp shell waste via microwave irradiation," *Process Saf. Environ. Prot.*, vol. 104, pp. 395-405, 2016, <https://doi.org/10.1016/j.psep.2016.09.020>
- (33) D. Montroni, M. Di Giosia, M. Calvaresi, and G. Falini, "Supramolecular Binding with Lectins: A New Route for Non-Covalent Functionalization of Polysaccharide Matrices," *Molecules*, vol. 27, no. 17, 2022, <https://doi.org/10.3390/molecules27175633>



- (34) K. Mohan, A. Ramu, and T. Muralisankar, "Trends in Food Science & Technology Recent insights into the extraction , characterization , and bioactivities of chitin and chitosan from insects," Trends Food Sci. Technol., vol. 105, no. May, pp. 17-42, 2020, <https://doi.org/10.1016/j.tifs.2020.08.016>
- (35) M. B. de O. Silva, S. A. de Oliveira, y D. dos S. Rosa, "Comparative study on microwave-assisted and conventional chitosan production from shrimp shell: Process optimization, characterization, and environmental impacts", J. Clean. Prod., vol. 440, no January, p. 140726, 2024. <https://doi.org/10.1016/j.jclepro.2024.140726>
- (36) I. Younes, S. Hajji, V. Frachet, M. Rinaudo, K. Jellouli, y M. Nasri, "Chitin extraction from shrimp shell using enzymatic treatment. Antitumor, antioxidant and antimicrobial activities of chitosan", Int. J. Biol. Macromol., vol. 69, pp. 489-498, 2014. <https://doi.org/10.1016/j.ijbiomac.2014.06.013>
- (37) R. S. C. M. D. Q. Antonino et al., "Preparation and characterization of chitosan obtained from shells of shrimp (Litopenaeus vannamei Boone," Mar. Drugs, vol. 15, no. 5, pp. 1-12, 2017, <https://doi.org/10.3390/md15050141>
- (38) Y. C. Cárdena-Pérez, R. Vera-Graziano, E. d. J. Muñoz-Prieto, and E. Y. Gómez-Pachón, "Obtención y caracterización de andamios electrohilados a base de quitosano y fibroína del capullo (Bombyx mori)," Ing. y Compet., vol. 19, no. 1, p. 134, 2017, <https://doi.org/10.25100/iyc.v19i1.2138>